Introduction to SEELab (ExpEYES 17)

Gayatri P
3rd year, Integrated M.Sc. Physics
Roll No.: 2211185
(Dated: April 1, 2025)

This report presents the results of a series of electronics experiments conducted using SeeLab, a hardware-software integration tool. The experiments included analyzing the output characteristics of an NPN transistor, studying the performance of different 555 multi-vibrator circuits, validating Faraday's and Lenz's laws, observing the emf dependence on the velocity of a falling magnet, estimating g using a rod pendulum and a phototransistor, and visualising sound beats. The experiments were designed to explore various concepts in electronics and demonstrate the capabilities of SeeLab as a flexible and versatile tool for hands-on learning and experimentation. The results obtained provide insights into the behavior of electronic circuits and validate fundamental electromagnetic principles.

I. OBJECTIVES

1. Study NPN Transistor Output Characterstics
2. Study Astable multivibrator with IC 555
3. Determine magnetic moment using EM induction
4. Determination of acceleration due to gravity g using Rod pendulum and a phototransistor
5. Study sound beats produced by two sources with nearly equal frequencies

II. THEORY

The ExpEYES-17 board is powered and interfaced with a computer's USB port, and it can be programmed using Python. It serves as a versatile tool with multiple functionalities, including a low-frequency oscilloscope, function generator, programmable voltage source, frequency counter, and data logger. The accompanying software enables monitoring and control of voltages at various terminals. Additionally, other parameters such as temperature, pressure, etc., can be measured by converting them into electrical signals using appropriate sensor elements.

A. NPN Transistor Output characteristics (CE)

The transistor functions by using a small current in one circuit to control a larger current in another circuit. The common emitter configuration is widely used in many applications. By studying the relationships between voltages and currents at different terminals, we can understand the transistor's operation. We plot the output characteristics by measuring the collector voltage against the collector current in a common emitter configuration, varying the base current. The collector current is determined from the voltage across a $1k\Omega$ resistor in the collector circuit.

The software controls the base current by adjusting the voltage at one end of the $1k\Omega$ resistor, with the other end connected to the transistor base. The base current value is calculated using the formula:

$$I_b = \frac{V_{PV2} V_{A2}}{100 \times 10^3} \times 10^6 \mu A \tag{1}$$

where V_{PV2} is the voltage at PV2 and V_{A2} is the voltage at A2. If A2 is not connected, the code assumes $0.6V$ at the base to calculate the base current.

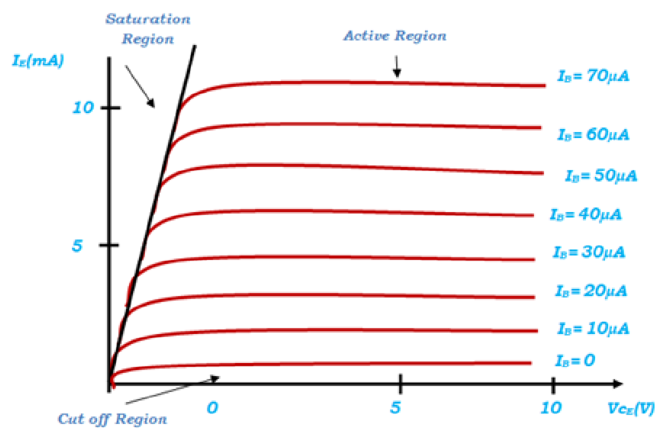

FIG. 1: Typical NPN output characterstics highlighting the sataration and active regions of the transistor

B. Astable multivibrator

A Multivibrator is a circuit that oscillates between a "HIGH" and "LOW" state, typically with a 50% duty cycle, meaning it has equal "ON" and "OFF" times. In sequential logic circuits, the state change may occur on the rising edge, falling edge, or both of the clock signal. On the other hand, stable pulse generation circuits do not have stable states, but rather continuously switch between two states, resulting in a train of square wave pulses at a fixed frequency. These concepts are important in understanding the behavior of multivibrators and pulse generation circuits, and play a significant role in digital electronics and circuit design.

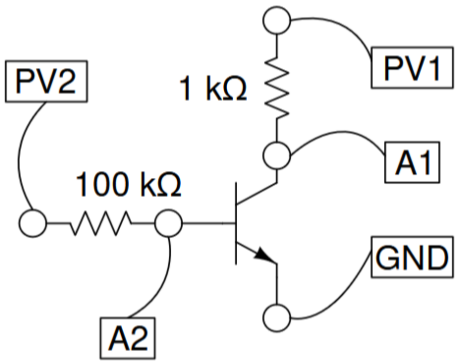

FIG. 2: Circuit diagram for observing the output characteristics of an NPN transistor in CE mode

The IC 555 is a popular integrated circuit with 23 transistors, two diodes, and 16 resistors, offering stability and affordability for timer and multivibrator applications. It can operate in mono/bi-stable or astable mode depending on external connections, generating single pulses or continuous pulse trains. Its versatility and characteristics make it widely used in modern electronics.

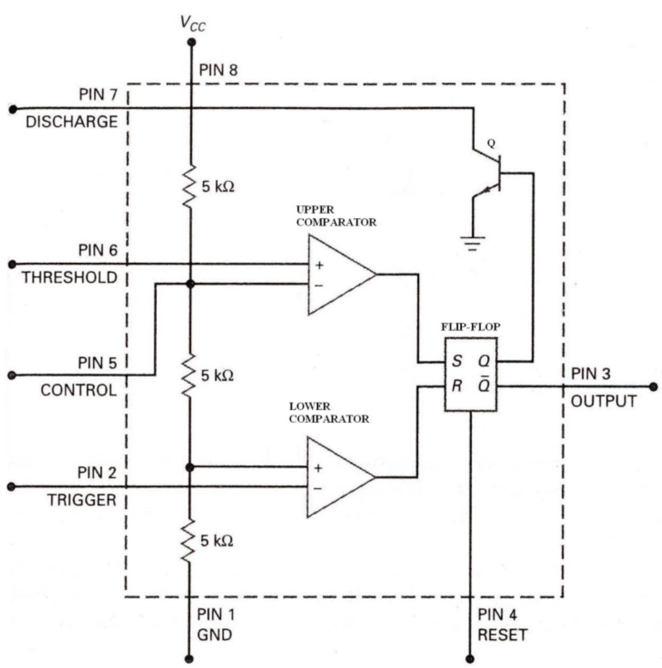

FIG. 3: Functional block diagram of IC 555

These circuits exhibit instability in any state and trigger output changes after specific time periods. As a result, they generate continuous square/rectangular waveforms with characteristics determined by the values of external resistors and capacitors.

The circuit diagrams in Figure 4 and Figure 5 depict the design of astable multivibrator using IC 555, with typical component values. The astable function is achieved by charging or discharging a capacitor through resistors connected to either V_{cc} or GND. The switching between charging and discharging modes is controlled by a resistor divider $(R_A - R_B)$, two comparators, and an RS flip-flop within the IC 555. The upper and lower comparators generate positive pulses when the voltage across the capacitor (V_C) exceeds $\frac{2}{3}V_{cc}$ or falls below $\frac{1}{3}V_{cc}$, respectively. These positive pulses then set or reset the Q output.

The astable multivibrator generates a continuous square or rectangular waveform with a duty cycle of 50% or more. The charging and discharging of the capacitor is controlled by the resistors and capacitors connected to the IC 555, which determine the frequency and duty cycle of the output waveform. The resistor values of R1 and R2, along with the capacitor value, determine the frequency of the output waveform, while the resistor values of R1 and R3 determine the duty cycle. By adjusting these resistor and capacitor values, the frequency and duty cycle of the output waveform can be varied to suit the desired application.

- The time for charging C from $\frac{1}{3}$ to $\frac{2}{3}$ V_{cc} (i.e, ON Time $= 0.693(R_A + R_B) \cdot C$)
- The time for discharging C from $\frac{2}{3}$ to $\frac{1}{3}$ V_{cc}, (i.e., OFF Time $= 0.693R_B \cdot C$)

To get the total oscillation period, adding the two:

$$\begin{aligned} T_{osc} &= 0.693(R_A + R_B)C + 0.693(R_B)C \\ &= 0.693 \cdot (R_A + 2 \cdot R_B) \cdot C \end{aligned} \tag{2}$$

$$f_{osc} = \frac{1}{T_{osc}} = \frac{1.44}{(R_A + 2R_B) \times C} \tag{3}$$

$$Duty - cycle = \frac{R_A + R_B}{R_A} + 2 \times R_B \tag{4}$$

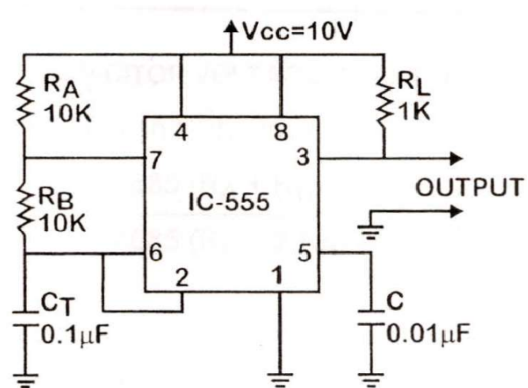

FIG. 4: Astable multivibrator circuit with duty cycle less than 50%

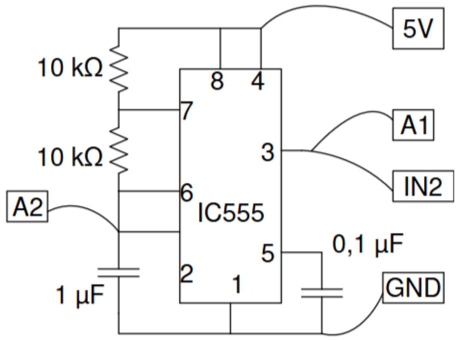

FIG. 5: Astable multivibrator circuit with the SEELab circuit pins highlighted

C. EM induction

Faraday's law of EM induction states that anytime the flux connected with a coil changes, an emf is induced in the coil; the direction is determined by Lenz's law and is proportional to the rate of change in flux linkage. Thus, the coil develops an eddy current as a result of this emf. Moving a magnet back and forth across a coil can alter the flux flowing through it. Here, we talk about the scenario when the coil is fixed and the magnet is lowered through it. Unless there is some additional mechanism, air resistance and gravity forces will cause the magnet's velocity to vary. If we drop the magnet vertically along the z-direction keeping the coil at the origin,

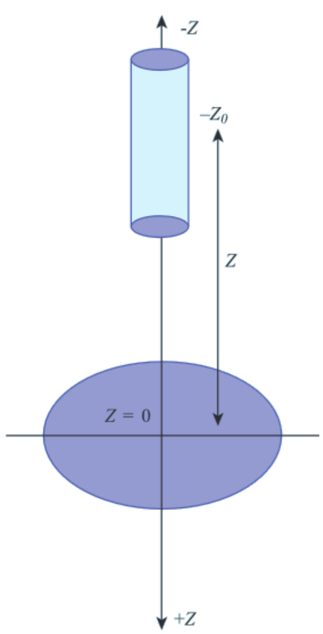

FIG. 6: A schematic representation of a magnet falling vertically through a coil.

$$z = -z_0 + 0.5gt^2$$
$$v = gt$$

where z_0 is the initial position of the magnet. Here g is the acceleration of the magnet. On passing through the coil, g decreases due to eddy current damping. Eddy current damping is responsible for the time delay in magnets falling through a long conductor. If the coil is short, we can neglect this. So the emf will be:

$$\begin{aligned} emf &= -N\frac{d\phi}{dt} \\ &= -N\frac{d(BA)}{dt} \end{aligned}$$

The coil's induced voltage can be expressed as $V = -NAB\sin(\theta)$, where A is the coil's area, N is the number of turns of the coil, and B is the magnetic field produced by the small cylindrical bar magnet at the coil's center. The magnet, with a dipole moment m, can be considered as a current-carrying loop with n turns if its length is small.

$$m = nIA = nI\pi R^2$$

where R is the radius of the cylindrical magnet. We know that the field along the axis of the circular coil at distance x is given by:

$$B = \frac{\mu_o m}{2\pi}(R^2 + x^2)^{-3/2}$$

thus emf is given by:

$$emf = \frac{3\mu_o m}{2\pi} NA(R^2 + x^2)^{-5/2} xv$$

where v is the velocity of the magnet, thus for non-constant velocity emf is given by,

$$\begin{aligned} emf = \frac{3\mu_o m}{2\pi} & NA(-z_0 + 0.5gt^2)gt \\ & \times (R^2 + (-z_0 + 0.5gt^2)^2)^{-5/2} \end{aligned} \tag{5}$$

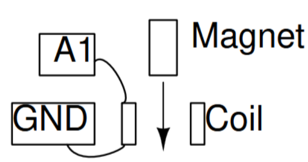

FIG. 7: Circuit diagram for EM induction

D. Determination of acceleration due to gravity using Rod pendulum

Period of oscillations of a pendulum depends on it's length and the value of gravity. Period of oscillation of a uniform rod about one end is given by

$$T = 2\pi\sqrt{\frac{2l}{3g}} \tag{6}$$

where l is the length and g is the acceleration due to gravity.

In this experiment, we measure the period of oscillations of a rod pendulum using a photo-transistor and LED arrangement. The pendulum (T-shaped, a knife edge attached to a 6mm diameter rod) is made to swing between an LED and photo-transistor, connected to expEYES. The LED and photo-transistor are mounted on a U-shaped bracket as shown in Fig. 8.

FIG. 8: Rod pendulum, photo-transisor and LED arrangement

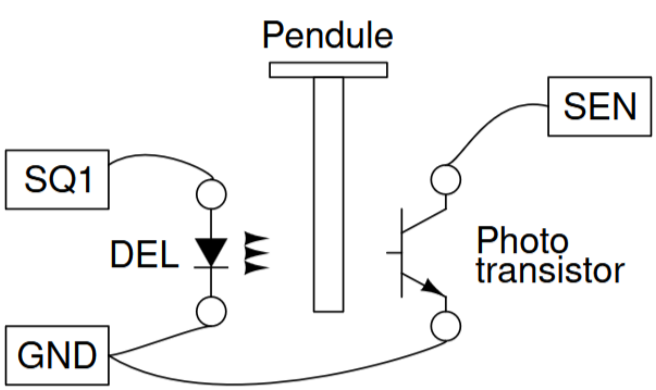

FIG. 9: Circuit diagram for the determination of g

E. Sound Beats produced by Two Sources with Nearly Equal Frequencies

Beats are produced when two sinusoidal sound waves of equal amplitude and very nearly equal frequencies mix. When two sound waves of nearly equal frequencies travel in the same direction, at a given point due to their superposition, the intensity alternatively increases and decreases periodically. This periodic waxing and winging of sound at a given position are called beats.

$$\cos(2\pi f_1 t) + \cos(2\pi f_2 t) = 2\cos\left(2\pi\frac{f_1+f_2}{2}t\right)\cos\left(2\pi\frac{f_1-f_2}{2}t\right)$$

The second cosine term in the above equationi acts as an envelope for the first cosine series with a reduced frequency of $f_b = f_1 - f_2$. This is what we percieve as sound beats.

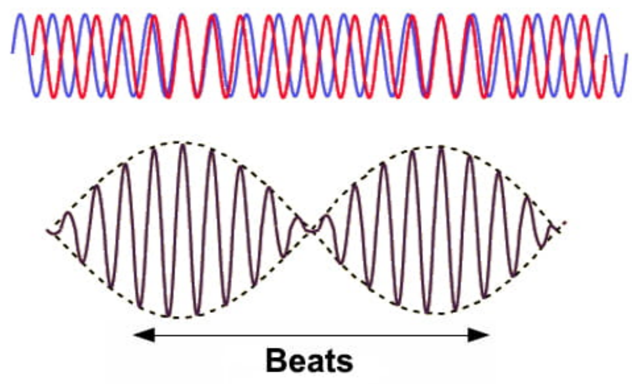

FIG. 10: Two waveforms of nearly equal frequency (above) in superposition, creates the below waveform with an overall envelope

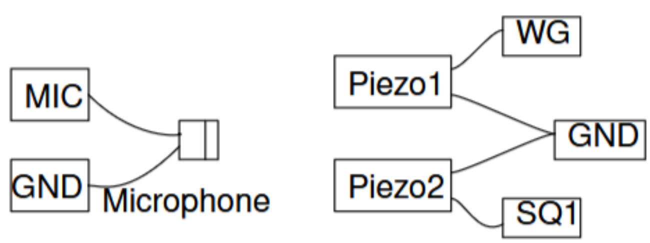

FIG. 11: Circuit Diagram for observing sound beats

III. EXPERIMENTAL SETUP

Apparatus

1. SEELab 3 Module

2. EXPEYES17 SEELab3 software
3. NPN transistor
4. IC 555 timer
5. Coil (with number of turns = 5000)
6. Small magnet (which fits through the coil)
7. A Rod Pendulum (T-shaped, with a knife edge attached to a 6mm diameter rod)
8. Phototransistor
9. Piezo buzzers
10. Microphone
11. Capacitors
12. Resistors
13. Connecting Wires
14. Power Supply

IV. OBSERVATION AND CALCULATION

The appendix includes all the screenshots of the SEELab3 software used in the following sections.

A. Transistor characteristics

The following figure shows the obtained output characteristics of the given NPN transistor.

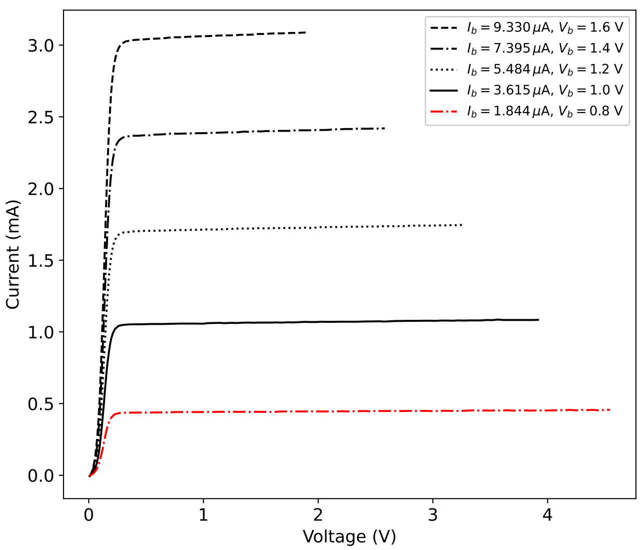

FIG. 12: Current vs. Voltage Output characteristics of an NPN transistor in CE mode

B. Astable multivibrator with IC 555

We have tested the astable multivibrator circuit for three different resistor combinations as give below.

1. $f \approx 1.2$ kHz

- $R_A = 10$ kΩ, $R_B = 1$ kΩ
- $C_T = 96.8$ nF

Parameter	Theoretical Value	Observed Value	Error
f_{osc}	1239.7 ± 0.6 Hz	1230.4 Hz	−0.3%
Duty Cycle	91.6 ± 0.02 %	91.7%	−0.1%

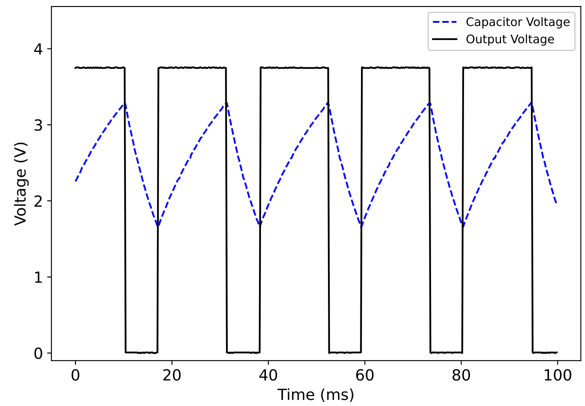

FIG. 13: Voltage vs time graph for Astable multivibrator with parameters given above

2. $f \approx 496$ Hz

- $R_A = 10$ kΩ, $R_B = 10$ kΩ
- $C_T = 96.8$ nF

Parameter	Theoretical Value	Observed Value	Error
f_{osc}	495.9 ± 0.3 Hz	487.2 Hz	−0.1%
Duty Cycle	33.3 ± 0.01 %	31.8%	−0.5%

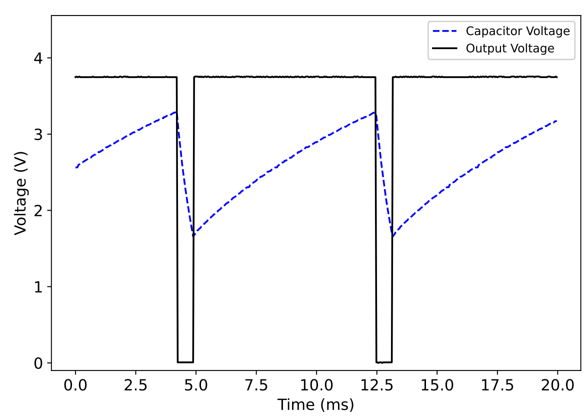

FIG. 14: Voltage vs time graph for Astable multivibrator with parameters given above

3. $f \approx 120$ *Hz*

- $R_A = 100$ kΩ, $R_B = 10$ kΩ
- $C_T = 96.8$ nF

Parameter	Theoretical Value	Observed Value	Error
f_{osc}	123.9 ± 0.7 Hz	119.7 Hz	-0.2%
Duty Cycle	83.3 ± 0.05 %	91.7%	-8.7%

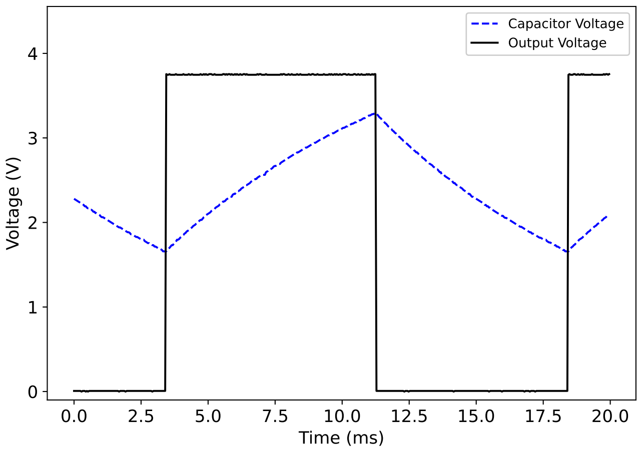

FIG. 15: Voltage vs time graph for Astable multivibrator with parameters given above

C. EM induction

The emf vs. time graphs for the magnet dropped at two different heights while the coil was fixed just above the ground is shown below.

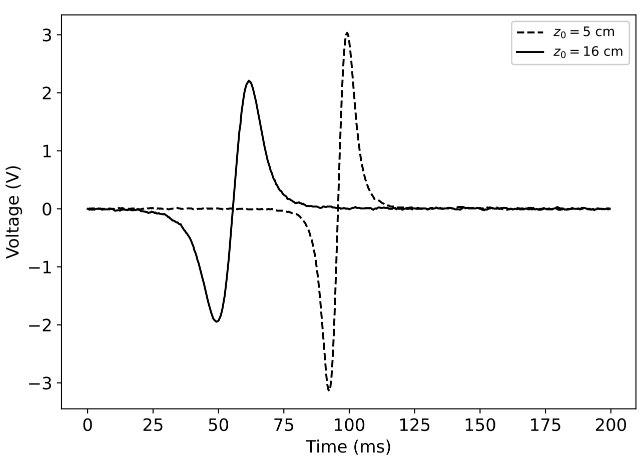

FIG. 16: Emf versus time graph for a vertically dropping magnet

From Equation 5 we have

We know that: z_o = initial position of the magnet. Also given: $N = 5000$, $R = 0.002m$ For both the cases,

- $z_0 = 5$ cm, $t = 115$ ms, $emf = 3.139$ V This gives us $m = 7.61$ Am^2.
- $z_0 = 16$ cm, $t = 181$ ms, $emf = 2.208$ V This gives us $m = 9.97$ Am^2.

Thus, $m = 8.79$ Am^2

D. Determination of g using Rod Pendulum

The period of oscillation of the pendulum rod has been measured here with an accuracy of 100 μs.

S.No.	Time (ms)
0	520.280
1	520.545
2	520.199
3	520.390
4	519.956
5	520.428
6	519.872
7	520.264
8	519.822
9	520.096
10	519.858

TABLE I: Table of the period of oscillation of the pendulum rod measured as it passes by the phototransistor

From this, the average value of $T_{avg} = 520.155$ ms. Plugging this is Eq. 6 (with $l = 10$ cm),

$$520.155 \times 10^{-3} = 2\pi\sqrt{\frac{2 \times 10 \times 10^{-2}}{3g}}$$
$$\implies g = 9.728 \text{ m/s}^2$$

E. Sound Beats

Below is the visualisation of the sound beats produced by the combination of two sounds of frequency 3400 Hz and 3500 Hz respectively.

Here, the time period of the small oscillations have been observed to be $T_1 = 0.29$ ms which equates to $f = 3448.2$ Hz. Similarly, the time period of the envelope is observed to be roughly $T_2 = 10.2$ ms which equates to $f_b = 98.1$ Hz. This is roughly equal to the theoretical value of $f = (f_1 + f_2)/2 = 3450$ Hz and $f_b = (f_1 - f_2) = 100$ Hz.

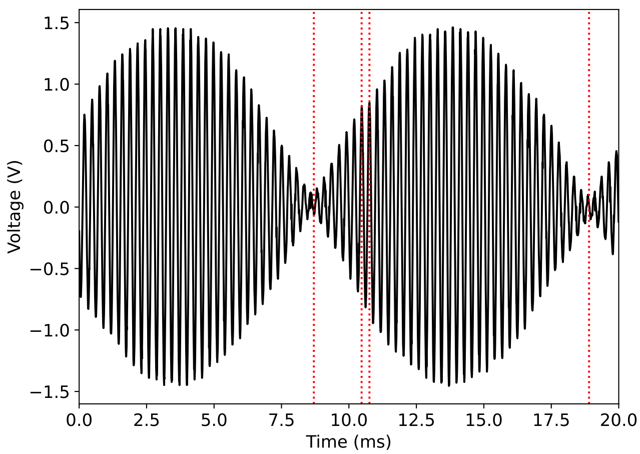

FIG. 17: Voltage versus time graph observed b a microphone sensor.

V. ERROR ANALYSIS

A. Astable Multivibrator

In $IC555$ multivibrator circuit the observed value of frequency and duty cycle is different from the theoretical value.

There may be several reasons for the high error in the observed values of frequency and duty cycle in the circuit using IC555. One possible reason is the difference between the actual values of resistors and capacitors used in the circuit and the ideal values assumed during calculations, which can affect the frequency and duty cycle. Another factor could be a loose connection or instability in the circuit, resulting in variations in the observed values.

The percentage errors in the calculated values have been mentioned in the previous section. The uncertainity in the theoretical values have been derived using the error propagation formula.

B. EM Induction

Similarly, the calculated magnetic moment may also have errors. Other forces such as air resistance and Lenz force, which are neglected in the calculations, could contribute to the error. Additionally, inaccuracies in the measured values of resistance (R) and distance (z) used in the calculations can also lead to errors in the magnetic moment value.

The uncertainity in the measurement of m can be derived using the error propagation formula, using the uncertainity in z_0 which is 0.1 cm and the uncertainity in V which is 0.001 V. Δm comes out to be 0.05 and 0.11 for $z_0 = 5$ and 16 cm respectively.

C. Determination of g using Rod Pendulum

The standard deviation of T_{avg} from Table I is measured to be $\Delta T = 0.252$ ms. Hence by using error propagation, we can find the uncertainity in measurement of g using

$$
\begin{aligned}
\frac{\Delta g}{g} &= \frac{2\Delta T}{T_{avg}} \\
\implies \Delta g &= 9.728 \times \frac{0.252}{520.155} \\
&= 0.005 \text{ m/s}^2
\end{aligned}
$$

where we assume $\Delta l = 0$. Hence, we have achieved remarkable precision in the measurement of g here.

In summary, the high error in the observed values of frequency, duty cycle, and magnetic moment may be attributed to various factors, incluing differences in actual component values, circuit instability, neglected forces, and inaccuracies in measured values.

VI. DISCUSSION & CONCLUSION

1. The NPN characteristics graph showed expected results, with the collector current remaining constant for a given base current, independent of the collector voltage above the threshold voltage of the Base-collector region.
2. The Multi-vibrator graph also matched the expected behavior in both cases, although there were slight errors in observed frequency and duty cycle values due to resistance and capacitance tolerances.
3. The EM wave graph exhibited two opposite peaks at different times, with the second peak being larger than the first peak. This indicates that the induced emf depends on the velocity of the magnet, with a higher moment of the magnet resulting in a larger emf. Negligible effects from Lenz's law and buoyant force were observed, and the magnetic moment of the magnet was calculated to be (8.79 ± 0.12) Am^2.
4. We were able to estimate the acceleration due to gravity using a rod pendulum and a phototransistor, chich came out to be remarkably close to the literature value, $g = (9.728 \pm 0.005)$ m/s^2. Let us also note that g can slightly vary from place to place.
5. We were also able to observe sound beats produced by the superposition of two sound waves of nearl equal frequencies. The sound and beat frequencies were observed to be $f = 3448.2$ Hz and $f_b = 98.1$ Hz respectively, which are about 0.001% and 0.02% deviated from the theoretical values.

VII. PRECAUTIONS AND SOURCES OF ERROR

1. For the rod pendulum, the length is measured from the knife edge to the bottom and used in the formula. But there is a small mass projecting above the knife edge that is not included in the calculation. Also the calculations assume that the pendulum must be exactly vertical in the resting position, which has to be ensured.
2. Make sure that the amplitudes of the two sound waves are nearly equal.

Appendix A: Screenshots from the Software

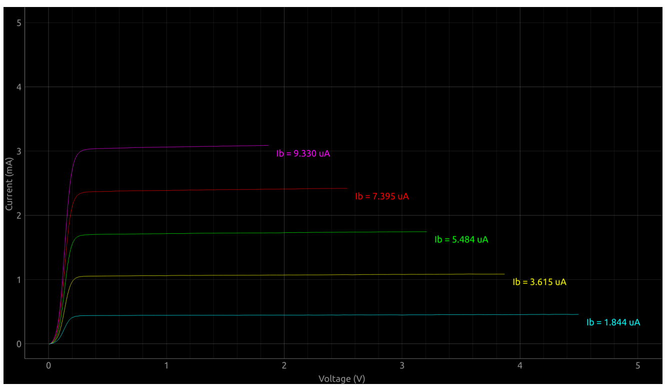

FIG. 18: NPN characteristics

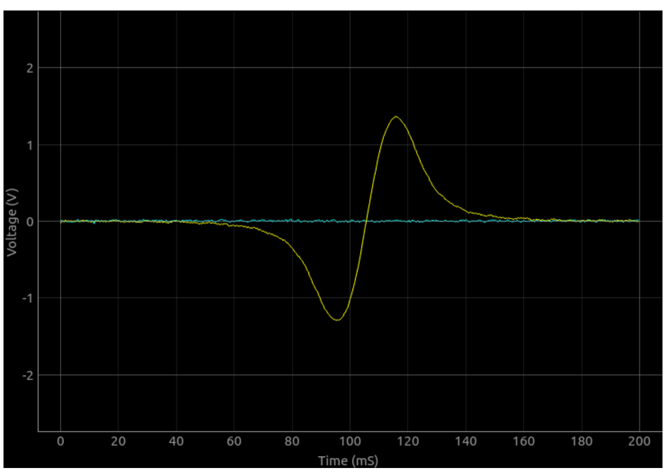

FIG. 19: emf produced by a falling magnet on a coil

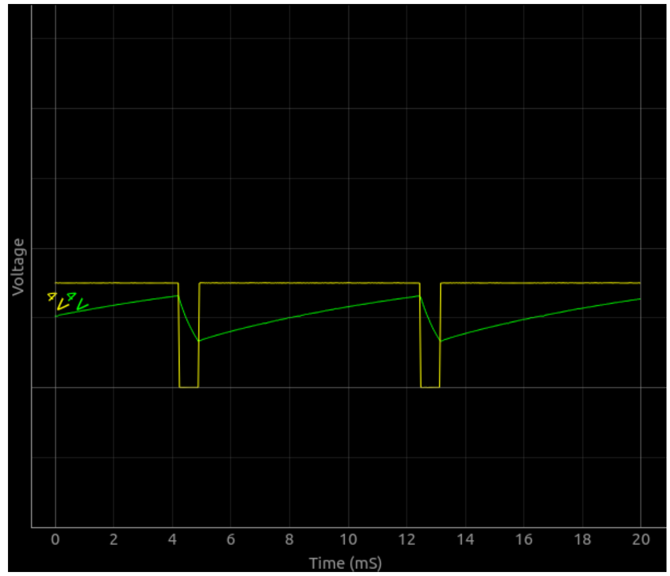

FIG. 20: Astable Multivibrator

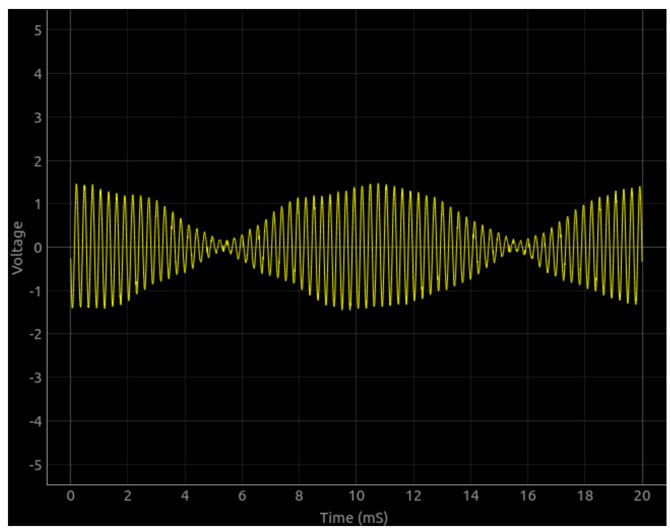

FIG. 21: Beats produced by two sound waves of nearly equal frequencies

[1] *expEYES-17 User Manual*, Projet PHOENIX, Inter-University Accelerator Centre (2022).
[2] K. M. N. Maryam, EM induction experiment to determine the moment of a magnet, Physics Education **49**, 319 (2014).